of hydrogen peroxide (H_2O_2) and horseradish peroxidase (HRP), respectively [13]. In this study, the HRP concentration was optimized to be at 0.124 units/ml with a gel point around 120 s, in order that the solution of hydrogel precursors would be injectable during the time interval and any uncontrolled diffusion of IFN-α2a after the injection could be avoided or minimized *in situ*. The storage modulus (G') of HA-Tyr hydrogels was 990 Pa and 3078 Pa when the H_2O_2 concentrations were 437 and 728 μM, respectively (Table 1). The significant difference in G' indicated that the stiffness of hydrogels could be tuned with H_2O_2 concentrations. IFN-α2a-incorporated HA-Tyr hydrogels were prepared and characterized in a similar manner. No significant differences were observed in G' between IFN-α2a-incorporated hydrogels and their counterparts without IFN-α2a, which indicates the IFN-α2a incorporation did not interfere with gel formation.

The crosslinking density and mesh size (ε) of the hydrogels were determined based on the measurements of the swelling ratio of hydrogels (Table 1). The crosslinking density of HA-Tyr-soft-IFN was lower than that of HA-Tyr-stiff-IFN while the mesh size of HA-Tyr-soft-IFN gel was significantly larger than that of HA-Tyr-stiff-IFN. Importantly, there was no significance in crosslinking density and mesh size of hydrogels with and without IFN-α2a, which further proved that the incorporation of the protein drug had very minimal effects on the hydrogel formation.

3.2. Release profiles of IFN-α2a from HA-Tyr hydrogels

The concentration of intact IFN-α2a released from hydrogels was determined by ELISA. We observed an initial rapid release of IFN-α2a from HA-Tyr hydrogels (Fig. 1). This rapid release was considered to be due to the protein's concentration difference across the interior of the hydrogel and its external environment [16]. As shown in Table 1, the mesh sizes of HA-Tyr-soft-IFN and HA-Tyr-stiff-IFN were 577 and 407 nm, respectively. As the hydrodynamic radius of IFN-α2a was 2.73 nm [26], and the mesh sizes of the HA-Tyr hydrogels were larger in two orders, that suggests IFN-α2a would diffuse freely within the gel matrix. Indeed, a linear plot was obtained by plotting release of IFN-α2a during the first 8 h as a function of the square root of time, which indicated a typical Fickian diffusion with first order release kinetics (Fig. 1 inset) [14]. The cumulative releases of IFN-α2a from HA-Tyr-soft-IFN and HA-Tyr-stiff-IFN after 8 h reached a plateau and were 78.5 ± 1.4% and 46.0 ± 1.7%, respectively (Fig. 1). In a separate study, freshly prepared HA-Tyr-IFN hydrogels were completely degraded by hyaluronidase *in vitro*. Then, we measured the concentration of IFN-α2a by ELISA. We found that 80.1 ± 0.8% and 56.0 ± 10.6% of IFN-α2a were retrieved from HA-Tyr-soft-IFN and HA-Tyr-stiff-IFN, respectively. These results indicate that the incomplete drug release from HA-Tyr hydrogels was considered to be due to the denaturation of IFN-α2a during crosslinking reaction. In addition, the results suggest that almost all the intact IFN-α2a could be released from HA-Tyr hydrogels by diffusion mechanism without the degradation of hydrogels.

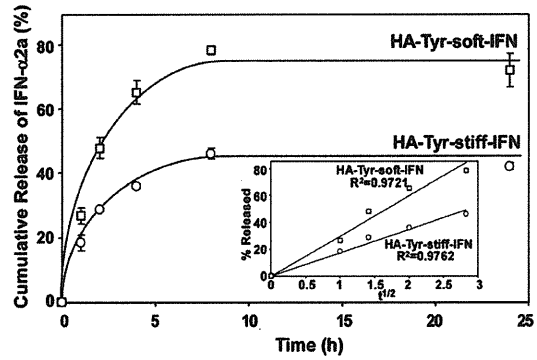

Fig. 1. Cumulative release of IFN-α2a from HA-Tyr-IFN hydrogels ($n = 3$, mean ± standard deviation). The inset shows the cumulative release of protein as a function of the square root of time.

3.3. Effects of crosslinking reaction on the activity of IFN-α2a incorporated in HA-Tyr hydrogels

The activity of IFN-α2a incorporated in the HA-Tyr hydrogel was investigated by an anti-viral assay in Huh-7 cells containing subgenomic Hepatitis C virus (HCV) replicon I_{389}luc-ubi-neo/NS3-3/5.1 [23]. When 2 pg/ml IFN-α2a was used, we found that the inhibition percentages of the viral RNA replication of the IFN-α2a retrieved from PBS, HA-Tyr-soft-IFN and HA-Tyr-stiff-IFN were 29 ± 3, 25 ± 2 and 12 ± 0.4, respectively (Fig. 2). The difference of inhibition percentages between IFN-α2a alone and HA-Tyr-soft-IFN was not statistically significant ($P = 0.11$), indicating the activity of IFN-α2a was well-maintained in HA-Tyr-soft-IFN. In contrast, IFN-α2a retrieved from HA-Tyr-stiff-IFN showed significantly lower activity compared to IFN-α2a solution. The results were further confirmed by using a different dose of IFN-α2a (4 pg/ml). These results clearly demonstrate that it is critical to choose the proper concentration of hydrogen peroxide utilized in the gelation to preserve the activity of the protein in the hydrogel. For HA-Tyr-soft-IFN, a high activity of IFN-α2a was maintained.

3.4. Inhibition of HAK-1B cell proliferation and induction of apoptosis upon treatment with IFN-incorporated HA-Tyr hydrogels

The HAK-1B cell line was established from a single nodule of hepatocellular carcinoma and has been confirmed to retain the morphological and functional characteristics of the original tumor [22]. As shown in Fig. 3a, the viability of HAK-1B was greater than 90% when HA-Tyr hydrogels without IFN-α2a were utilized, indicating the hydrogels are non-cytotoxic. We observed that the percentages of viable cells after treatment with IFN-α2a solution, HA-Tyr-soft-IFN and HA-Tyr-stiff-IFN were 25, 42 and 59, respectively. As we have confirmed the activity of IFN-α2a in HA-Tyr-soft-IFN was similar to that of IFN-α2a solution

Table 1
Characterization of IFN-α2a-incorporated HA-Tyr hydrogels[a].

Sample	H_2O_2 (μM)	G' (Pa)	Q_M	Q_V	ν_e (10^{-6} mol/cm^3)	ε (nm)
HA-Tyr-soft	437	990 ± 49	46.1 ± 0.5	56.4 ± 0.7	1.8 ± 0.04	546.8 ± 7.6
HA-Tyr-soft-IFN	437	898 ± 122[b]	48.3 ± 2.5	59.1 ± 3.0	1.7 ± 0.1[c]	576.8 ± 34.6[d]
HA-Tyr-stiff	728	3078 ± 184	39.3 ± 1.5	48.1 ± 1.9	2.4 ± 0.2	453.2 ± 20.7
HA-Tyr-stiff-IFN	728	3028 ± 199[b]	35.8 ± 2.3	43.8 ± 2.8	2.8 ± 0.3[c]	406.5 ± 30.5[d]

Note. Results are shown as the mean values ± standard deviation ($n = 3$). Abbreviations: storage modulus (G'), mass swelling ratio (Q_M), volumetric swelling ratio (Q_V), effective crosslink density (ν_e), mesh size (ε).

[a] All hydrogels were formed with 1.75 wt.% of HA-Tyr conjugate and 0.124 units/ml of HRP with or without 2.5×10^5 IU/ml of IFN-α2a.

[b] G', [c]ν_e and [d]ε of HA-Tyr hydrogels with IFN-α2a were not significantly different from those of HA-Tyr hydrogels without IFN-α2a ($P > 0.05$).

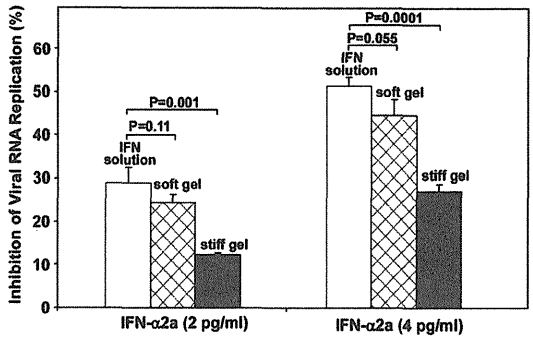

Fig. 2. Anti-viral activity of IFN-α2a retrieved from HA-Tyr-IFN hydrogels after treatment with 250 U/ml hyaluronidase ($n=3$, mean ± standard deviation).

(Section 3.3), the significant difference in cell viability between IFN-α2a solution and HA-Tyr-soft-IFN would be attributed to the prolonged release of IFN-α2a from hydrogels in cell culture.

After treatment with the IFN-α2a or IFN-α2a-incorporated hydrogels, the percentages of live cells dropped significantly as compared to the control (Fig. 3b). On the other hand, the percentages of apoptotic and dead cells increased after treatment with IFN-α2a or IFN-α2a-incorporated hydrogels. The percentages of apoptotic cells treated with IFN-α2a or HA-Tyr-soft-IFN were significantly higher than that of HA-Tyr-stiff-IFN (Table 2). Meanwhile there was no significantly different percentage of apoptotic cells between groups treated by IFN-α2a and HA-Tyr-soft-IFN. These results indicated that HAK-1B cells were undergoing apoptosis after treatment with IFN-α2a-incorporated hydrogels and further confirmed that the activity of IFN-α2a was well-maintained in HA-Tyr-soft-IFN.

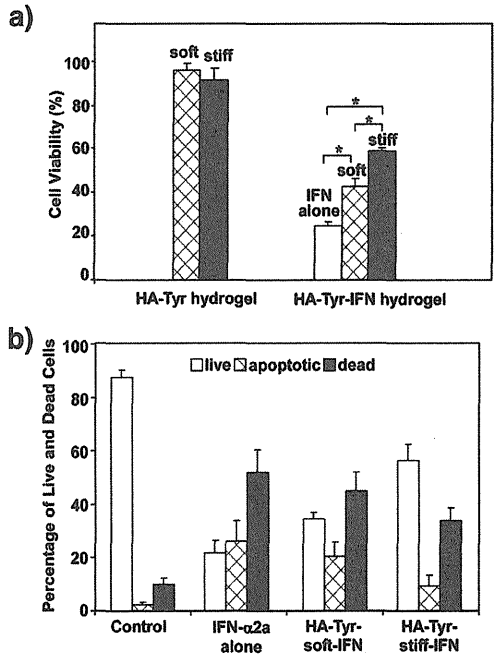

Fig. 3. (a) The viability of HAK-1B cells measured by alarmarBlue assay after 4-day treatment of HA-Tyr hydrogels with or without 4×10^5 IU/ml of IFN-α2a. *: $P<0.05$. (b) Ratio of live/apoptotic/dead HAK-1B cells after treatment of HA-Tyr hydrogels with IFN-α2a (4×10^5 IU/ml) ($n=3$, mean ± standard deviation).

3.5. Caspase-3/7 activity of HAK-1B cells upon treatment with IFN-incorporated HA-Tyr hydrogels

We examined the intracellular activity of caspase-3/7 to investigate the mechanism of apoptosis in HAK-1B after hydrogel treatment. After treatment with IFN-α2a or IFN-α2a-incorporated HA-Tyr hydrogels, the HAK-1B cells showed red fluorescence for active caspase-3/7, whereas cells without treatment showed little staining (Fig. 4a). HA-Tyr-soft-IFN-treated cells showed stronger staining of caspase-3/7 than the HA-Tyr-stiff-IFN-treated cells. Furthermore, the co-staining of caspase-3/7 with cell nuclei in cells treated with the IFN-α2a solution or HA-Tyr-soft-IFN, indicated that those cells were in late stage apoptosis as caspase-3/7 would translocate into nuclear after proteolytic activation and substrate recognition [27]. On the other hand, most of caspase-3/7 stains in HA-Tyr-stiff-IFN-treated cells remained in cytoplasm, indicating an early stage of apoptosis in these cells.

We utilized the Apo-ONE capspase-3/7 assay kit to quantify caspase-3/7 activity in HAK-1B cells after treatment. As shown in Fig. 4b, cells without any treatment showed low fluorescence intensity that indicated there was minimal amount of active caspase-3/7 in the healthy cells. HA-Tyr-soft-IFN-treated cells showed lower fluorescence intensity than IFN-α2a-solution-treated cells, due to the slow release of IFN-α2a from the hydrogel in culture media. On the other hand, HA-Tyr-stiff-IFN-treated cells showed less than half of the fluorescence intensity of HA-Tyr-soft-IFN-treated cells. Such a sizably lower fluorescence intensity is considered to be due to the decreased activity and slower release rate of IFN-α2a from HA-Tyr-stiff-IFN. These results were consistent with the confocal images, and demonstrated that the released IFN-α2a from HA-Tyr hydrogels activated caspase-3/7 in HAK-1B cells.

3.6. Pharmacokinetics of IFN-α2a in the plasma and delivered IFN-α2a in the tumor of mice

We performed the pharmacokinetics study of circulating IFN-α2a in the plasma of mice. As shown in Fig. 5a, at 1 h post injection the concentration of IFN-α2a in the plasma of mice treated with IFN-α2a solution, HA-Tyr-soft-IFN and HA-Tyr-stiff-IFN was 105, 35 and 47 ng/ml, respectively. The high concentration IFN-α2a in the plasma of IFN-α2a-solution-treated mice suggested that the subcutaneously injected IFN-α2a got into the circulation rapidly. In contrast, the concentration of IFN-α2a in the plasma of hydrogel-treated mice was much lower than that of IFN-α2a solution, that indicated a slow release of the protein from the hydrogels at 1 h. From 1 h to 4 h, the concentration of IFN-α2a in the plasma of IFN-α2a solution-treated mice decreased rather rapidly (2 h: 65 ng/ml, 4 h: 8 ng/ml). In contrast, the hydrogel-treated mice plasma showed much slower decreases of IFN-α2a concentrations (HA-Tyr-soft-IFN: 2 h at 30 ng/ml, 4 h at 26 ng/ml; HA-Tyr-stiff-IFN: 2 h at 32 ng/ml, 4 h at 17 ng/ml), that suggested there was a continuous release of IFN-α2a from both types of hydrogels. At 8 h, the concentration of IFN-α2a became negligible in IFN-solution-treated mice, whereas the protein concentration was 8 ng/ml for hydrogel-treated mice. These results clearly

Table 2
Statistical analysis of percentages of live/apoptotic/dead cells upon treatment with IFN-α2a-incorporated HA-Tyr hydrogels[a].

ANOVA test	Live	Apoptotic	Dead
Control vs. HA-Tyr-soft-IFN	**	**	**
Control vs. HA-Tyr-stiff-IFN	**	*	**
IFN-α2a vs. HA-Tyr-soft-IFN	**	*	*
IFN-α2a vs. HA-Tyr-stiff-IFN	**	*	
HA-Tyr-soft-IFN vs. HA-Tyr-stiff-IFN			

[a] Statistical analysis was performed using one-way ANOVA and Student's t test.
* $P<0.05$.
** $P<0.01$.

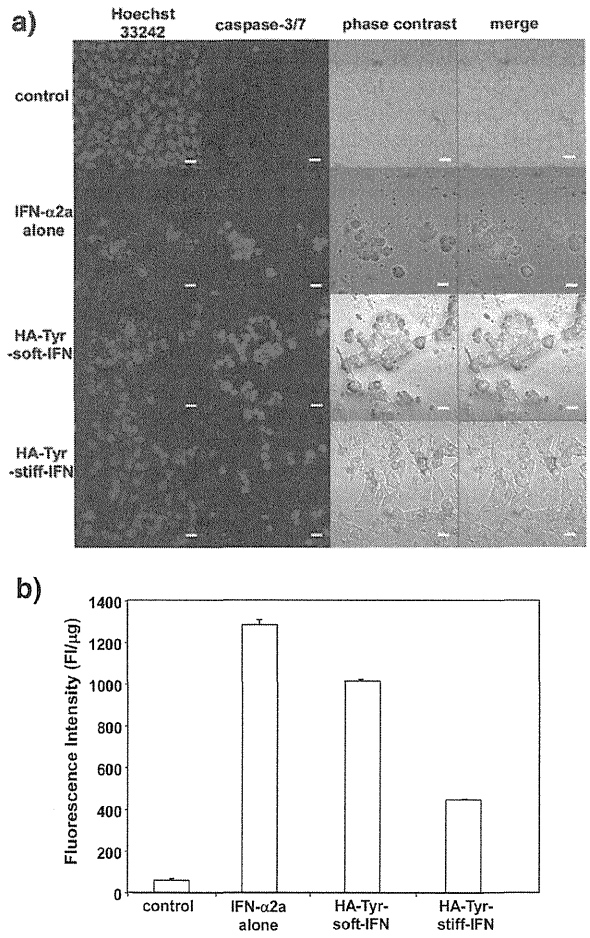

Fig. 4. (a) Confocal images of HAK-1B cells after treatment of HA-Tyr-IFN hydrogels. Cells were stained with Hoechst 33342 (blue) and SR-DEVD-FMK FLICA (red) and pictures were taken with a confocal machine Zeiss LSM 5 DUO. (b) Quantitative measurement of caspase 3/7 activity in cells treated with HA-Tyr-IFN hydrogels. Cells were harvested after treatment and Promega Apo-ONE Homogeneous caspase-3/7 assay as well as BCA protein assay was performed. The results were presented as fluorescence intensity (FI) normalized with the total protein amount (μg) in each sample ($n=3$, mean ± standard deviation). (For interpretation of the references to color in this figure legend, the reader is referred to the web version of the article.)

demonstrated prolonged and continuous release of IFN-α2a from HA-Tyr hydrogels *in vivo*.

Next, we examined the amount of IFN-α2a that was delivered at the tumor site. At 8 h post injection, the delivered amount of IFN-α2a at the tumor site of HA-Tyr-soft-IFN-treated mice was around 1200 pg per gram of tumor tissue, that was three-fold the amount for the IFN-α2a-solution-treated mice (Fig. 5b). The delivered amount of IFN-α2a in HA-Tyr-stiff-IFN-treated mice was two-fold to the delivery for IFN-α2a solution-treated mice. Overall, the IFN-α2a-incorporated hydrogels showed enhanced delivery of the protein drug at the tumor site when compared to protein solution injection.

3.7. Anticancer effect in tumor-xenografted nude mice

The anticancer effect of IFN-α2a-incorporated HA-Tyr hydrogels was examined *in vivo* using a HAK-1B-xenografted nude mouse model. Each group of mice ($n=7$) received subcutaneous injections of HA-Tyr-IFN or IFN-α2a solution. PBS and hydrogels without IFN-α2a were also injected as controls. Fig. 6a shows that the treatment of HA-Tyr hydrogels without

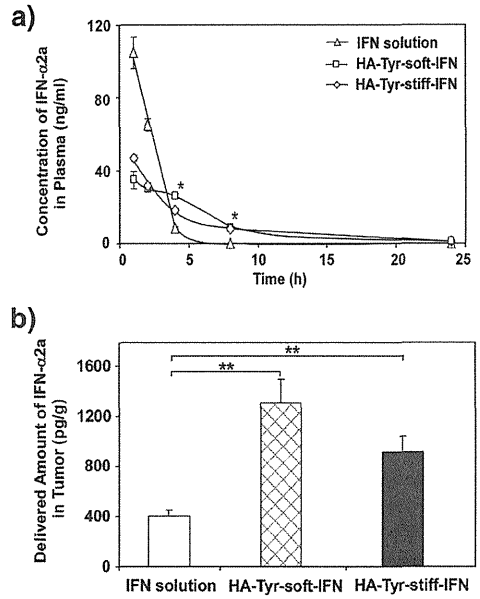

Fig. 5. (a) Pharmacokinetics of IFN-α2a in the plasma of Balb/c nude mice ($n=3$, mean ± standard error of the mean). *: $P<0.05$. (b) Amount of IFN-α2a delivered to tumor tissues of HAK-1B inoculated Balb/c nude mice. The amount of IFN-α2a (pg) delivered at the tumor tissue was normalized with the weight of the tumor (g) ($n=4$, mean ± standard error of the mean). **: $P<0.01$.

IFN-α2a showed no significant effect in tumor regression, that indicates the hydrogel itself has no anti-tumor efficacy. The treatment with IFN-α2a solution did not prevent the growth of tumors as average tumor size in the IFN-α2a solution group was not significantly different

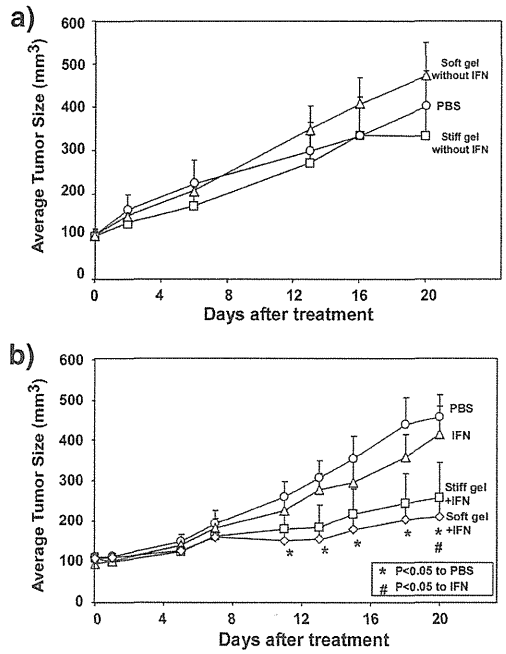

Fig. 6. (a) Tumor regression study of HAK-1B inoculated Balb/c nude mice treated with PBS or HA-Tyr hydrogels without IFN-α2a. (b) Tumor regression study of HAK-1B inoculated Balb/c nude mice treated with PBS, IFN-α2a solution or HA-Tyr-IFN hydrogels ($n=7$, mean ± standard error of the mean).

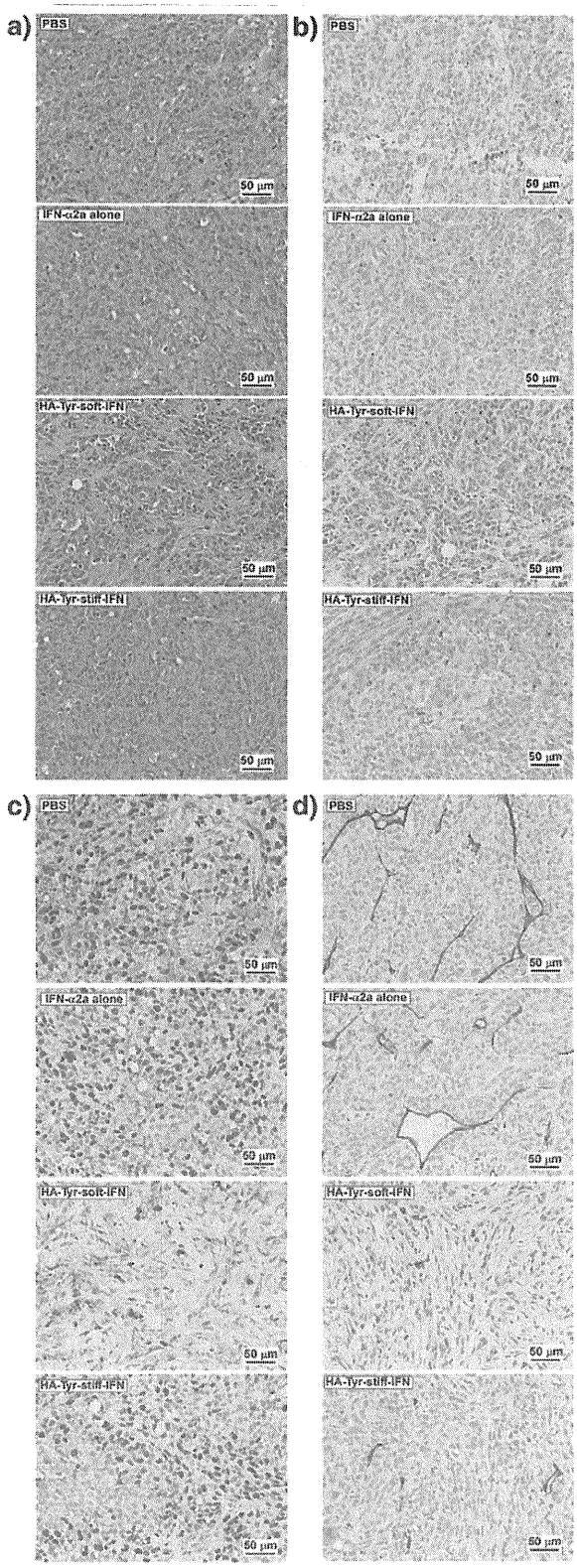

from the PBS group in 20 days (Fig. 6b). In contrast, the groups treated with IFN-α2a-incorporated HA-Tyr hydrogels showed a remarkable decrease in average tumor size. In the group of HA-Tyr-soft-IFN-treated mice, the average tumor size was significantly lower than that of PBS control from day 11 onward ($P<0.05$), that suggested the delivered IFN-α2a from HA-Tyr-soft-IFN effectively inhibited the growth of tumors in mice. We also observed a similar trend of decreasing tumor size in HA-Tyr-stiff-IFN-treated mice, although there was no significant difference in the average tumor size between these mice and PBS control. Thus, IFN-α2a-incorporated HA-Tyr hydrogels have enhanced anti-tumor efficacy in the tumor regression study. In addition, there were minimal side-effects caused by the injection of HA-Tyr hydrogels, as the hydrogel-treated mice maintained their weight and no dead mice were found during the period of study. Also, we did not observe any dead mice from the group without hydrogel-treatment.

We further investigated the histological changes of tumor tissues for the mice treated with IFN-α2a-incorporated hydrogels. Fig. 7a shows the hematoxylin and eosin (H & E) staining of tumor sections from the mice that were treated with PBS, IFN-α2a alone or IFN-α2a-incorporated hydrogels. The nuclei density of tumor cells in HA-Tyr-soft-IFN-treated mice was lower than that of other groups, which was consistent with the results from tumor regression, and confirmed that the treatment with HA-Tyr-soft-IFN showed high antitumor efficacy. Then, we examined the intracellular markers of apoptosis and proliferation in the tumor sections of hydrogel-treated mice. Terminal deoxynucleotidyl transferase dUTP nick end labeling (TUNEL) staining showed a high ratio of apoptotic cells in tumor sections of mice that were treated with HA-Tyr-soft-IFN and HA-Tyr-stiff-IFN (Fig. 7b), that indicated more tumor cells were undergoing apoptosis after treatment with the IFN-α2a-incorporated hydrogels when compared to tumor cells from the PBS group or IFN-α2a solution group. Ki 67 staining revealed an obvious decrease of positive cells in tumor sections in hydrogel-treated mice as compared to the control (Fig. 7c). Since Ki67 is a nuclear protein associated with cellular proliferation [28], it indicated that the tumor cells in HA-Tyr-soft-IFN-treated mice had stopped proliferation and were under senescence. From these results, we summarized that tumor cells were apoptotic and less proliferative in HA-Tyr-soft-IFN-treated mice, while tumor cells were highly proliferative in IFN-α2a-solution-treated mice.

Antiangiogenesis therapy is one of the most significant advances in cancer research [29]. As IFN has been reported to show antiangiogenesis effects in hepatocellular carcinoma [30], we proceeded to examine the angiogenesis of tumor sections of mice after treatment with IFN-α2a-incorporated hydrogels through staining with CD34, which is a cell surface glycoprotein that has been reported as a marker for angiogenesis in cancer [31]. Fig. 7d shows the CD34 staining in the tumor sections of mice that were treated with PBS, IFN-α2a solution or IFN-incorporated hydrogels. In the tumor sections of mice that were treated with PBS or IFN-α2a solution, we observed the positive staining of CD34 with linear, semicircular and circular patterns, indicating an extensive distribution of blood vessels in those samples. In contrast, we only found a few CD34 stains in tumor sections of mice that were treated with IFN-α2a-incorporated hydrogels. This result suggested that angiogenesis was efficiently inhibited in mice that were treated with IFN-incorporated hydrogels.

4. Conclusion

We have demonstrated an injectable IFN-α2a-incorporated HA-Tyr hydrogel system for liver cancer therapy. IFN-α2a-incorporated HA-Tyr hydrogels with tunable stiffness and rapid gelation rate were

Fig. 7. Histological examinations of tumor tissues from HAK-1B inoculated Balb/c nude mice. (a) H & E, (b) TUNEL (brown), (c) Ki67 (brown) and (d) CD34 (brown). (For interpretation of the references to color in this figure legend, the reader is referred to the web version of the article.)

prepared using an enzyme-mediated oxidative coupling reaction involving the Tyr moiety of the HA-Tyr conjugate. The incorporation of IFN-α2a did not change the gelation properties of the hydrogels; the activity of the incorporated protein was well-maintained when a lower concentration of H_2O_2 (437 μM) was used. The release of IFN-α2a from the hydrogels was shown to occur by diffusion *in vitro*. IFN-α2a released from the hydrogels inhibited the proliferation of HAK-1B liver cancer cells, and induced apoptosis through caspase-3/7 pathway. *In vivo* studies revealed that treatment of IFN-α2a-incorporated hydrogels showed improved pharmacokinetics in the plasma of mice, and up to three-fold of IFN-α2a was delivered at the tumor site compared to delivery via IFN-α2a solution injection. In the tumor regression study, treatment with the HA-Tyr-soft-IFN hydrogel reduced the average tumor size significantly from day 11 onwards, while injection with IFN-α2a alone failed to provide antitumor efficacy. Furthermore, histological and immunohistochemical analyses showed lower cell density in tumors after treatment with HA-Tyr-soft-IFN hydrogel, with more apoptotic cells and less proliferating cells as compared to tumors in animals treated with PBS or IFN solution. In addition, angiogenesis was efficiently inhibited in tumors that were treated with IFN-α2a-incorporated hydrogels. Therefore, we provide an alternative approach to improve the anticancer efficacy of protein drugs in liver cancer therapy by using an injectable hydrogel system that incorporates protein therapeutics. We believe that such an approach could be applied to other protein drugs for the treatment of various diseases in the future.

Acknowledgments

This work was supported by the Institute of Bioengineering and Nanotechnology (Biomedical Research Council, Agency for Science, Technology and Research, Singapore). The authors wish to thank JNC Corporation, Japan, for the gift of hyaluronic acid and Prof. Ralf Bartenschlager, University of Heidelberg, Germany, for providing the Huh-7 cells containing subgenomic HCV replicon I_{389}luc-ubi-neo/NS3-3/5.1 with adaptive mutation.

References

[1] G. Walsh, Biopharmaceutical benchmarks 2010, Nat. Biotechnol. 28 (2010) 917–924.
[2] B. Leader, Q.J. Baca, D.E. Golan, Protein therapeutics: a summary and pharmacological classification, Nat. Rev. Drug Discov. 7 (2008) 21–39.
[3] A.C. Chan, P.J. Carter, Therapeutic antibodies for autoimmunity and inflammation, Nat. Rev. Immunol. 10 (2010) 301–316.
[4] L.M. Weiner, R. Surana, S. Wang, Monoclonal antibodies: versatile platforms for cancer immunotherapy, Nat. Rev. Immunol. 10 (2010) 317–327.
[5] N. Lonberg, Fully human antibodies from transgenic mouse and phage display platforms, Curr. Opin. Immunol. 20 (2008) 450–459.
[6] R.E. Kontermann, Strategies for extended serum half-life of protein therapeutics, Curr. Opin. Biotechnol. 22 (2011) 868–876.
[7] W.H. Vogel, Infusion reactions: diagnosis, assessment, and management, Clin. J. Oncol. Nurs. 14 (2010) E10–E21.
[8] A.S. Hoffman, Hydrogels for biomedical applications, Adv. Drug Deliv. Rev. 54 (2002) 3–12.
[9] L.S. Wang, J.E. Chung, P.P.Y. Chan, M. Kurisawa, Injectable biodegradable hydrogels with tunable mechanical properties for the stimulation of neurogenesic differentiation of human mesenchymal stem cells in 3D culture, Biomaterials 31 (2010) 1148–1157.
[10] W.S. Toh, T.C. Lim, M. Kurisawa, M. Spector, Modulation of mesenchymal stem cell chondrogenesis in a tunable hyaluronic acid hydrogel microenvironment, Biomaterials 33 (2012) 3835–3845.
[11] M. Kurisawa, J.E. Chung, Y.Y. Yang, S.J. Gao, H. Uyama, Injectable biodegradable hydrogels composed of hyaluronic acid-tyramine conjugates for drug delivery and tissue engineering, Chem. Commun. 14 (2005) 4312–4314.
[12] M. Kurisawa, F. Lee, L.S. Wang, J.E. Chung, Injectable enzymatically crosslinked hydrogel system with independent tuning of mechanical strength and gelation rate for drug delivery and tissue engineering, J. Mater. Chem. 20 (2010) 5371–5375.
[13] F. Lee, J.E. Chung, M. Kurisawa, An injectable enzymatically crosslinked hyaluronic acid-tyramine hydrogel system with independent tuning of mechanical strength and gelation rate, Soft Matter 4 (2008) 880–887.
[14] F. Lee, J.E. Chung, M. Kurisawa, An injectable hyaluronic acid-tyramine hydrogel system for protein delivery, J. Control. Release 134 (2009) 186–193.
[15] X.Z. Shu, Y.C. Liu, F.S. Palumbo, Y. Lu, G.D. Prestwich, In situ crosslinkable hyaluronan hydrogels for tissue engineering, Biomaterials 25 (2004) 1339–1348.
[16] S. Cai, Y. Liu, X. Zheng Shu, G.D. Prestwich, Injectable glycosaminoglycan hydrogels for controlled release of human basic fibroblast growth factor, Biomaterials 26 (2005) 6054–6067.
[17] C.M. Nimmo, S.C. Owen, M.S. Shoichet, Diels–Alder click cross-linked hyaluronic acid hydrogels for tissue engineering, Biomacromolecules 12 (2011) 824–830.
[18] J.H. Hoofnagle, K.D. Mullen, D.B. Jones, V. Rustgi, A. Dibisceglie, M. Peters, J.G. Waggoner, Y. Park, E.A. Jones, Treatment of chronic non-A, non-B Hepatitis with recombinant human alpha-interferon — a preliminary report, N. Engl. J. Med. 315 (1986) 1575–1578.
[19] A.U. Neumann, N.P. Lam, H. Dahari, D.R. Gretch, T.E. Wiley, T.J. Layden, A.S. Perelson, Hepatitis C viral dynamics in vivo and the antiviral efficacy of interferon-alpha therapy, Science 282 (1998) 103–107.
[20] H. Yano, A. Iemura, M. Haramaki, S. Ogasawara, A. Takayama, J. Akiba, M. Kojiro, Interferon alfa receptor expression and growth inhibition by interferon alfa in human liver cancer cell lines, Hepatology 29 (1999) 1708–1717.
[21] T. Hisaka, H. Yano, S. Ogasawara, S. Momosaki, N. Nishida, Y. Takemoto, S. Kojiro, Y. Katafuchi, M. Kojiro, Interferon-alpha Con1 suppresses proliferation of liver cancer cell lines in vitro and in vivo, J. Hepatol. 41 (2004) 782–789.
[22] H. Yano, A. Iemura, K. Fukuda, A. Mizoguchi, M. Haramaki, M. Kojiro, Establishment of 2 distint human hepatocellular carcinoma cell lines from a single nodule showing clonal dedifferentiation of cancer cells, Hepatology 18 (1993) 320–327.
[23] J.M. Vrolijk, A. Kaul, B.E. Hansen, V. Lohmann, B.L. Haagmans, S.W. Schalm, R. Bartenschlager, A replicon-based bioassay for the measurement of interferons in patients with chronic hepatitis C, J. Virol. Methods 110 (2003) 201–209.
[24] T. Pietschmann, M. Zayas, P. Meuleman, G. Long, N. Appel, G. Koutsoudakis, S. Kallis, G. Leroux-Roels, V. Lohmann, R. Bartenschlager, Production of infectious genotype 1b virus particles in cell culture and impairment by replication enhancing mutations, PLoS Pathog. 5 (2009) 14.
[25] J.B. Leach, K.A. Bivens, C.W. Patrick, C.E. Schmidt, Photocrosslinked hyaluronic acid hydrogels: natural, biodegradable tissue engineering scaffolds, Biotechnol. Bioeng. 82 (2003) 578–589.
[26] C. Dhalluin, A. Ross, L.A. Leuthold, S. Foser, B. Gsell, F. Muller, H. Senn, Structural and biophysical characterization of the 40 kDa PEG-interferon-alpha2a and its individual positional isomers, Bioconjug. Chem. 16 (2005) 504–517.
[27] S. Kamada, U. Kikkawa, Y. Tsujimoto, T. Hunter, Nuclear translocation of caspase-3 is dependent on its proteolytic activation and recognition of a substrate-like protein(s), J. Biol. Chem. 280 (2005) 857–860.
[28] J. Bullwinkel, B. Baron-Luhr, A. Ludemann, C. Wohlenberg, J. Gerdes, T. Scholzen, Ki-67 protein is associated with ribosomal RNA transcription in quiescent and proliferating cells, J. Cell. Physiol. 206 (2006) 624–635.
[29] N. Ferrara, R.S. Kerbel, Angiogenesis as a therapeutic target, Nature 438 (2005) 967–974.
[30] D. Ribatti, A. Vacca, B. Nico, D. Sansonno, F. Dammacco, Angiogenesis and anti-angiogenesis in hepatocellular carcinoma, Cancer Treat. Rev. 32 (2006) 437–444.
[31] M.-C. Bettencourt, J.J. Bauer, I.A. Sesterhenn, R.R. Connelly, J.W. Moul, CD34 immunohistochemical assessment of angiogenesis as a prognostic marker for prostate cancer recurrence after radical prostatectomy, J. Urol. 160 (1998) 459–465.

Article type: Original Article - Hepatology (Experimental)

Received date: 04-Apr-2013

Accepted date: 15-Nov-2013

Title: SP cell fractions from HCC cell lines increased with tumor dedifferentiation, but lack characteristic features of CSCs.

Masamichi Nakayama[1)2)], Sachiko Ogasawara[1)], Jun Akiba[1)], Kousuke Ueda[1)], Keiko Koura[1)2)], Keita Todoroki[1)], Hisafumi Kinoshita[2)], Hirohisa Yano[1)]

1) Department of Pathology, Kurume University School of Medicine, Kurume, Japan

2) Department of Surgery, Kurume University School of Medicine, Kurume, Japan

Corresponding author: Jun Akiba

Address: Department of Pathology, Kurume University School of Medicine,

67 Asahimachi, Kurume 830-0011, JAPAN

Tel: +81-942-31-7546

Fax: +81-942-32-0905

E-mail: akiba@med.kurume-u.ac.jp

Abstract

Background and Aim: Cancer stem cells (CSCs), a minority population with stem cell-like characteristics, play important roles in cancer development and progression. Putative CSC markers, such as CD13, CD90, CD133, and EpCAM, and side population (SP) technique are generally used in an attempt to isolate CSCs. We aimed to clarify the relationship between CSCs and clonal dedifferentiation in hepatocellular carcinoma (HCC).

Methods: We used a well-differentiated HCC cell line (HAK-1A) and a poorly differentiated HCC cell line (HAK-1B) established from a single nodule with histological heterogeneity. HAK-1B arose due to clonal dedifferentiation of HAK-1A. The SP cells and non-SP (NSP) cells were isolated from the two cell lines with a FACSAria II and used for the analyses.

Results: The SP cell fractions in HAK-1A and HAK-1B were 0.2% and 0.9%, respectively. CD90 or EpCAM was not expressed in either HAK-1A or HAK-1B, while CD13 and CD133 were expressed in HAK-1B alone. Although sphere forming ability, tumorigenicity, growth rate, and CD13 expression were higher in HAK-1B SP cells than HAK-1B NSP cells, there were no differences in drug resistance, colony forming ability, or cell cycle rates between HAK-1B SP and NSP cells, suggesting HAK-1B SP cells do not fulfill CSC criteria.

Conclusions: Our findings suggested a possible relationship between the expression of CSC markers and clonal dedifferentiation. However, the complete features of CSC could not be identified in SP cells, and the concept of SP cells as a universal marker for CSC may not apply to HAK-1A and HAK-1B.

Keywords: cancer stem cells, side population cells, dedifferentiation

Introduction

Cancer stem cells (CSCs) are defined by self-renewing capacity, differentiation capacity, and tumor-initiating capacity. Additionally, the seeding of metastasis and tumor relapse are attributed to CSCs [1-3]. To date, the existence of CSCs has been proven not only in hematopoietic neoplasms [4, 5], but also various solid neoplasms [6-11].

Side population (SP) cell sorting was initially applied for the identification of hematopoietic stem cells and has been used to enrich stem cell compartments in diverse tissues and organs [12-14]. SP cells are detected by their ability to efflux Hoechst 33342 dye through ATP-binding cassette (ABC) membrane transporters. Recently, SP cells have also been used in an attempt to isolate a stem cell–like fraction in cancer cells [15-17]. The approach seems valuable because a variety of cancers, including HCC, highly express ABC transporters, which are reported to contribute to multi-drug resistance [18].

A variety of markers have been successfully used to enrich CSC fractions from different tumors including HCC [19]. Although no markers for putative liver CSCs have been generally accepted, CD133, CD90, epithelial cell adhesion molecule (EpCAM) and CD13 are thought to be candidates for liver CSC markers [20-24].

Recent evidence suggests that CSCs, a minority population with stem-cell-like characteristics, play important roles in cancer development and progression [25].

In this study, we isolated the SP and non-SP (NSP) cells from two HCC cell lines, a well-differentiated human HCC cell line (HAK-1A) and a poorly differentiated HCC cell line (HAK-1B) which were established from a single nodule with a three-layered structure having different histologic features [26], and compared the relationship between CSCs and clonal dedifferentiation.

Materials and methods

Cell lines and cell culture

This study used two human HCC cell lines: HAK-1A, HAK-1B, which were both established from a single HCC nodule showing a three-layered structure with a different histological grade in each layer [26]. HAK-1A resembles well-differentiated HCC cells in the outer layer of the original tumor, and HAK-1B resembles poorly differentiated cells in the inner layer. The presence of an identical point mutation in the p53 gene in the two cell lines suggests that they are of clonal origin. The cell culture condition is described elsewhere [26].

SP cell analysis using flow cytometry

We followed the protocol previously reported by Goodell et al. [13], with minor modifications. Briefly, cells were detached from the culture dish with Accutase (Innovative Cell Technologies, Inc., San Diego, CA, USA). The cells were incubated at 37 °C for 60 minutes with Hoechst 33342 (SIGMA-Aldrich, Saint Louis, MO, USA). The control cells were incubated in the presence of 15 μg Reserpine (SIGMA-Aldrich). After staining, the cells were suspended in PBS with 2% FBS, filtered through a 40 μm cell strainer (BD Biosciences, San Jose, CA, USA). Cells were counterstained with 0.5 μg/mL propidium iodide (PI, BD Biosciences) for the discrimination of dead cells. Viable cells were analyzed and isolated by a FACSAria II (BD Biosciences).

Immunofluorescence flow cytometric analysis of SP and NSP cells

We analyzed SP and NSP cells isolated from HAK-1A and HAK-1B for expression of the putative stem cell markers CD133, CD90, EpCAM and CD13. Cells were first stained with Hoechst 33342. Excess dye was removed by resuspending 1×10^6 cells/mL in PBS with 2% FBS. Cells were incubated in the dark at 4 °C for 30 minutes with fluorescence-conjugated monoclonal antibodies, including allophycocyanin (APC) -conjugated mouse anti human CD133/2 (293C3) antibodies (Miltenyi Biotec, Bergisch-Gladbach, Germany), fluorescein isothiocyanate (FITC) -conjugated mouse

anti human CD90, phycoerythrin (PE) -conjugated mouse anti human EpCAM and Purified Mouse Anti-Human CD13 (BD Biosciences). After 30 minutes, cells with Purified Mouse Anti-Human CD13 were also incubated in the dark at 4 °C for 30 minutes with Goat Anti-Mouse Ig FITC (BD Biosciences). Cells were counterstained with 0.5 μg/mL PI for the discrimination of dead cells. The data were analyzed using a FACSAria II.

Generation of SP and NSP cells by SP or NSP cells

A total of 1 x 10^5 sorted SP cells or NSP cells from HAK-1A and HAK-1B were cultured for 1 week, and used for SP cell analysis, as described above, to examine whether SP or NSP cells generate SP and NSP cells.

Proliferation of HAK-1B SP and NSP cells

The proliferative ability of the cells from each subpopulation, including HAK-1B SP and NSP cells was examined using colorimetric assays with 3-(4, 5-dimethylthiazol-2yl-yl-)-2, 5-dimethyl tetrazolium bromide (MTT) cell growth assay kits (Chemicon, Temecula, CA, USA), as described elsewhere [27]. SP and NSP cells (1500 cells/well) were seeded on 96-well plates (Falcon, Becton Dickinson Labware, Tokyo, Japan) by a FACS Aria II. After culture for 24 h, 48 h, 72 h, 96 h, or 120 h, the number of viable cells was examined.

Effects of CDDP, 5-FU, and PEG-IFN-α2b on the proliferation of HAK-1B SP and NSP cells

Effects of Cisplatin (CDDP) (Nihonkayaku, Tokyo, Japan), 5-fluorouracil (5-FU) (Kyowa Hakko, Tokyo, Japan) and pegylated IFN-α2b (PEG-IFN-α2b) (Schering-Plough K.K., Osaka, Japan) on cell proliferation were examined by MTT assay. SP and NSP cells (1,500 cells/well) were seeded on 96-well plates, cultured for 24 h, and then the culture

medium was replaced with a new medium containing CDDP alone (0, 0.125, 0.25 or 0.5 μg/mL); 5-FU alone (0, 0.75, 1.5 or 3 μM); or PEG-IFN-α2b (0, 500, 1,000 or 2,000 IU/mL). After culturing for 48 h or 96 h, the number of viable cells was examined by MTT assay.

Drug treatment assay of SP and NSP cells in HAK-1A and HAK-1B

HAK-1A and HAK-1B cells were cultured with medium alone (Control) or medium containing 5-FU (1.5 μM) or PEG-IFN-α2b (1,000 IU/mL) and cultured for 96 hours, and SP cell analysis, as described above, was performed to estimate the effect of drugs on SP cell fraction.

Cell cycle analysis of HAK-1B SP and NSP cells

Cultured HAK-1B cells were labeled with 10mM bromodeoxyuridine (BrdU) (Sigma Chemical Co., St. Louis, MO) for 30 min, harvested, and used for the isolation of SP and NSP by a FACSAria II. Isolated SP or NSP cells were used for cell cycle analysis according to the technique described elsewhere [28]. The percentage of the cells in the G_1, S or G_2/M phase was calculated from a dot plot.

Colony formation assay of HAK-1B SP and NSP cells

Colony formation assay was performed almost according to a modified previously described method [29]. The number of colonies > 0.5 mm in diameter was counted 14 days later.

Sphere formation assay of HAK-1B SP and NSP cells

We performed sphere formation assay according to a previously described method [29].

Tumorigenicity assay of HAK-1B SP and NSP cells *in vivo*

Various numbers of cells (1, 5, 10, 50, or 100 x 10^3) were injected subcutaneously into 4-week-old female NOD/SCID mice (n=5 in each group). Tumorigenic capacity was judged 8 weeks after injection. All procedures were approved by the Ethics Review Committee for Animal Experimentation of Kurume University School of Medicine.

Gene expression microarrays of SP and NSP cells isolated from HAK-1A and HAK-1B

The cRNA was amplified, labeled, and hybridized to a 44K Agilent 60-mer oligomicroarray according to the manufacturer's instructions. All hybridized microarray slides were scanned by an Agilent scanner. Relative hybridization intensities and background hybridization values were calculated using Agilent Feature Extraction Software (9.5.1.1).

Quantitative real-time reverse transcriptase-polymerase chain reaction (qRT-PCR) of SP and NSP cells isolated from HAK-1A and HAK-1B

Total RNA was extracted using RNeasy Plus Micro Kit (Qiagen, Valencia, CA, USA) and complementary DNA (cDNA) was synthesized using Reverse Transcription System (Promega, Madison, WI, USA) according to the manufacturer's instructions. qRT-PCR was carried out with TaqMan technology using ABI PRISM 7500 (Applied Biosystems, Foster City, CA, USA) followed by a previously published method [29]. Gene expression assays primer and probe mixes were used for CD13, CD133, CD24, CD44, CD90, EpCAM, ABCG2, Oct-4, Nanog, BMI1, Alb, CYP3A4 and β-actin (assay IDs are listed in Table 1; Applied Biosystems).

Statistical analysis

Comparison of colorimetric cell growth, drug resistance, colony forming ability and sphere forming ability were performed using Student's *t*-test. Differences were considered significant at $P<0.05$.

Results

1. Identification of SP and NSP cells in HAK-1A and HAK-1B and expression of CSC markers

The SP cell fraction in HAK-1A was very low at only 0.2%. Expression of the putative CSC markers, such as CD133, CD90, EpCAM, CD13, was almost completely absent in both SP and NSP cells from HAK-1A (Fig. 1a). The SP fraction in HAK-1B was 0.9%. Moreover, while CD90 and EpCAM expression was absent in HAK-1B SP and NSP cells, CD133 expression was observed both in 4.6～6.4% of HAK-1B SP cells and in 3.9～5.3% of HAK-1B NSP cells. CD13 expression was higher in SP cells (21.7%) than in NSP cells (8.9%) (Fig. 1b).

2. Generation SP and NSP cells from sorted SP and NSP cells in HAK-1A and HAK-1B

After culturing HAK-1A SP cells or HAK-1B SP cells for 1 week, the percentage of HAK-1A and HAK-1B SP cells decreased to 1.9% and 7.3%, respectively. In contrast, culture of HAK-1A SP cells and HAK-1B NSP cells generated a small population of SP cells in HAK-1A (0.1%) and HAK1B (0.7%). The results suggest the SP cells could generate NSP cells, and vice versa (Fig. 2).

3. Biological features of SP and NSP cells in HAK-1B cells *in vitro*.

In HAK-1B, SP cell growth was significantly higher than that of NSP cells at every time point (24 h, 48 h, 72 h, 96 h, and 120 h; Fig. 3a). The cell cycle analysis revealed no obvious differences in G_0-G_1/ S/ G_2-M ratios between SP cells (64.0%/ 30.1%/ 4.2%) and NSP cells (65.3%/ 31.9%/ 1.6%) (Fig. 3b).

Drug resistance to 5-FU, CDDP or PEG-IFN-α2b was examined. The results showed that the viability of HAK-1B SP cells (58.7%) was significantly lower than that of HAK-1B NSP cells (71.5%) at 96 h in cells treated with 0.75 μM 5-FU (P<0.001).

Similarly, after 96 h treatment with 1.5 μM 5-FU, viability of SP cells fell to 40.7%, compared with 47.9% in NSP cells ($P<0.05$). SP cell viability was also significantly lower (50.7%) than NSP cells (63.5%)($P<0.05$) after 96 h treatment with 500 IU/mL PEG-IFN-α2b. No other significant differences were observed between SP and NSP cells (Fig. 3c). After exposure of HAK-1B cells to PEG-IFN-α2b for 72 h, the percentage of SP cells decreased as compared with control. Conversely, the percentage of SP cells increased when HAK-1B cells were treated with 5-FU for 72 h (Fig. 3d).

In the colony formation assay, SP cells from HAK-1B formed 252 ±33.4 colonies, while the NSP cells formed 243 ±70.1 colonies; this difference was not significant (Fig. 4a). Sphere formation was significantly higher in SP cells (21.0±4.1 spheres) as compared with NSP cells (15.7±2.7 spheres) in the HAK-1B cell line ($P<0.05$; Fig. 4b).

4. Biological features of SP and NSP cells in HAK-1B cells *in vivo*.

Injection of 1, 5, or 10 x 10^3 SP or NSP cells produced no tumors in NOD/SCID mice. In contrast, four mice that received 5 x 10^4 SP cells and five mice that received 10 x 10^4 SP cells developed tumors at 8 weeks. In addition, one mouse that received 5 x 10^4 NSP cells and two mice that received 10 x 10^4 NSP cells also developed small tumors (Fig.4c).

5. cDNA microarray analysis of gene expression in SP and NSP cells sorted from HAK-1A or HAK-1B cells

cDNA microarray analysis found 884 and 470 differences in gene expression between HAK-1A and HAK-1B, respectively, but there were no significant differences between SP and NSP cells in expression of stemness genes (e.g., CD44, Oct-4, Bim-1, ABCG2, CD24, EpCAM)(Table 2).

6. qRT-PCR analysis of SP and NSP cells in HAK-1A or HAK-1B cells

SP and NSP cells of HAK-1A and HAK-1B expressed mRNAs of CSC markers, such as

CD13, CD133, CD24, CD44, EpCAM, ABCG2, Nanog, and Bmi-1. The expression of these molecules was slightly higher in SP cells than in NSP cells. In addition, the differences in expression levels of CD133, CD24, and CD44 between SP and NSP cells were slightly larger in HAK-1B than HAK-1A cells (Fig. 4a and 4b). The other putative CSC markers, such as CD90 and Oct-4, were not expressed. As to hepatocyte markers, CYP3A4 was expressed in HAK-1A and HAK-1B, but albumin was not expressed in either cell line.

Discussion

The present study utilized two HCC cell lines showing clonal dedifferentiation that were established at our department from a single nodule-in-nodule HCC (HAK-1A, HAK-1B), and which are unique in the world. Our aim was to study the SP cell fractions, which are considered universal markers for CSCs [15-17], in these two cell lines to clarify the relationship between CSCs and clonal dedifferentiation

SP cells from HAK-1A, which was established from a part of the well-differentiated HCC, represented only 0.2% of total cells, an extremely low percentage. However, in SP cells from the HAK-1B cell line, which is a part of the poorly-differentiated HCC derived from dedifferentiation of HAK-1A, the SP fraction was 0.9%, 4.5 times higher than in HAK-1A. Further, our analysis of the putative CSCs markers CD133, CD90, EpCAM and CD13 found no expression of CD90 or EpCAM in either HAK-1A or HAK-1B, while CD13 and CD133 was expressed in HAK-1B alone. In addition, while there was no difference in the expression of CD133 between SP and NSP cells in HAK-1B, CD13 expression was apparently higher in HAK-1B SP cells (21.7%) than HAK-1B NSP cells (8.9%). Haraguchi et al. [20] have reported that CD13 was an abundantly expressed marker in SP cells from the HCC cell lines HuH7 and PLC/PRL/5. This fraction existed primarily during the G_0 phase of the cell cycle, and exhibited high tumorigenicity and drug resistance. Our findings suggest the possibility that CD13 could also be a CSC

marker for HAK-1B cells. The significance of CD13 in HAK-1B should be further studied.

Analysis of biological features revealed that HAK-1B SP cells possess some properties of CSC, such as higher sphere forming ability and tumorigenicity, as compared with NSP cells. However, HAK-1B SP cells lacked the following four features of CSC. Firstly, HAK-1B SP cells lacked high drug resistance and colony forming ability. Drug treatment usually increases the percentage of CSC, but our results did not always show such tendency, i.e., PEG-IFN-α2b treatment increased the percentage of SP cells, but 5-FU treatment increased the percentage of SP cells. The reason for this contradictory result is not clear and should be further elucidated. Secondly, the percentage of G_0/G_1 phase is usually higher in CSC, but our cell cycle analysis revealed no difference in rates between SP and NSP cells. Thirdly, differentiated cells do not generate CSC, but in our study, NSP cells could generate SP cells. Fourthly, no difference in microarray analysis and slight difference in qRT-PCR analysis were observed in stemness gene expression between SP and NSP cells.

These results suggest that HAK-1B SP cells do not fulfill the criteria to be considered CSCs.

As described above, it is recognized that the SP cell fraction in a variety of tumors is rich in CSC [15-17], but some reports question whether there is a relationship between SP cells and CSCs. Burket et al. [30] examined SP and NSP cells in 4 gastrointestinal cancer cell lines and found that CD34 was expressed in the NSP fraction but not in the SP fraction, however no significant differences were observed in any other category, including colony formation, tumorigenicity, or multi-lineage differentiation.

Two main theories are still being debated with regard to the histogenesis of HCC. For many years the observation of preneoplastic nodules in HCC induced experimentally by exposure to chemicals supported the dedifferentiation hypothesis, i.e. the theory that HCC was derived from the dedifferentiation of adult hepatocytes. Further, the recent

discovery of the role of small oval cells in the process of carcinogenesis has led to development of the maturation arrest hypothesis, which suggests that HCC derives from the maturation arrest of hepatic stem cells, and analysis of HCC cells has indicated the presence of cells with stem-cell-like properties [31]. It is also suspected that dedifferentiation may cause CSCs. As of yet there have been no reports on the relationship between dedifferentiation and CSCs. The present study suggested a relationship between dedifferentiation and expression of CSC markers, but many aspects of the mechanisms of dedifferentiation remain unclear, and many different mechanisms have been reported to explain the abnormal proliferation and dedifferentiation of liver cells in HCC pathogenesis. Among these the most common are (i) inactivation of p53, p14 and p16, (ii) overexpression of cyclin D1/Cdk4, insulin-like growth factor-II or c-MET, or (iii) activation of the Ras/mitogen activated protein kinase (MAPK), transforming growth factor (TGF)-β signaling or Wnt/β-catenin signaling [32-37]. Further studies are required to clarify the mechanisms underlying dedifferentiation, including the relation between dedifferentiation and CSCs.

In conclusion, the present study found that the SP cell fraction was 4.5 times higher in the HAK-1B cell line than in the HAK-1A cell line, and that the expression of CD13 and CD133, which are considered to be CSC markers, was observed only in HAK-1B. Also, a comparison of HAK-1B SP and NSP cells found that CD13 expression was higher in the SP fraction, suggesting a possible relationship between the expression of CSC markers and dedifferentiation. Moreover, HAK-1B SP cells showed more malignant biological features, such as higher sphere forming ability and tumorigenicity as compared with NSP cells. However, with the exception of these biological features, no other CSC characteristics were clearly observed in the HAK-1B SP cells. Thus, the concept of the SP cells as a universal marker for CSC may not apply to HAK-1A and HAK-1B. We plan to examine the relationship between dedifferentiation and CSC using other CSC markers, such as CD13 and CD133.

Acknowledgements

We thank Ms. Akemi Fujiyoshi for her excellent assistance in our experiments.

References

1. Clarke, M.F., et al., *Cancer stem cells--perspectives on current status and future directions: AACR Workshop on cancer stem cells.* Cancer Res, 2006. **66**(19):9339-9344.
2. Jordan, C.T., M.L. Guzman, and M. Noble, *Cancer stem cells.* N Engl J Med, 2006. **355**(12):1253-1261.
3. Marquardt, J.U., V.M. Factor, and S.S. Thorgeirsson, *Epigenetic regulation of cancer stem cells in liver cancer: current concepts and clinical implications.* J Hepatol. **53**(3):568-577.
4. Lapidot, T., et al., *A cell initiating human acute myeloid leukaemia after transplantation into SCID mice.* Nature, 1994. **367**(6464): 645-648.
5. Bonnet, D. and J.E. Dick, *Human acute myeloid leukemia is organized as a hierarchy that originates from a primitive hematopoietic cell.* Nat Med, 1997. **3**(7):730-737.
6. Collins, A.T., et al., *Prospective identification of tumorigenic prostate cancer stem cells.* Cancer Res, 2005. **65**(23):10946-10951.
7. Houghton, J., et al., *Gastric cancer originating from bone marrow-derived cells.* Science, 2004. **306**(5701):1568-1571.
8. Kim, C.F., et al., *Identification of bronchioalveolar stem cells in normal lung and lung cancer.* Cell, 2005. **121**(6):823-835.
9. Ponti, D., et al., *Isolation and in vitro propagation of tumorigenic breast cancer cells with stem/progenitor cell properties.* Cancer Res, 2005. **65**(13):5506-5511.
10. Ricci-Vitiani, L., et al., *Identification and expansion of human colon-cancer-initiating cells.* Nature, 2007. **445**(7123):111-115.
11. Singh, S.K., et al., *Identification of a cancer stem cell in human brain tumors.* Cancer Res, 2003. **63**(18):5821-5828.
12. Falciatori, I., et al., *Identification and enrichment of spermatogonial stem cells*

displaying side-population phenotype in immature mouse testis. FASEB J, 2004. **18**(2):376-378.

13. Goodell, M.A., et al., *Isolation and functional properties of murine hematopoietic stem cells that are replicating in vivo.* J Exp Med, 1996. **183**(4):1797-1806.
14. Shimano, K., et al., *Hepatic oval cells have the side population phenotype defined by expression of ATP-binding cassette transporter ABCG2/BCRP1.* Am J Pathol, 2003. **163**(1):3-9.
15. Kondo, T., T. Setoguchi, and T. Taga, *Persistence of a small subpopulation of cancer stem-like cells in the C6 glioma cell line.* Proc Natl Acad Sci U S A, 2004. **101**(3):781-786.
16. Chiba, T., et al., *Side population purified from hepatocellular carcinoma cells harbors cancer stem cell-like properties.* Hepatology, 2006. **44**(1):240-251.
17. Patrawala, L., et al., *Side population is enriched in tumorigenic, stem-like cancer cells, whereas ABCG2+ and ABCG2- cancer cells are similarly tumorigenic.* Cancer Res, 2005. **65**(14):6207-6219.
18. Itsubo, M., et al., *Immunohistochemical study of expression and cellular localization of the multidrug resistance gene product P-glycoprotein in primary liver carcinoma.* Cancer, 1994. **73**(2):298-303.
19. Park, C.Y., D. Tseng, and I.L. Weissman, *Cancer stem cell-directed therapies: recent data from the laboratory and clinic.* Mol Ther, 2009. **17**(2):219-30.
20. Haraguchi, N., et al., *CD13 is a therapeutic target in human liver cancer stem cells.* J Clin Invest. **120**(9):3326-3339.
21. Ma, S., et al., *Identification and characterization of tumorigenic liver cancer stem/progenitor cells.* Gastroenterology, 2007. **132**(7):2542-2556.
22. Suetsugu, A., et al., *Characterization of CD133+ hepatocellular carcinoma cells as cancer stem/progenitor cells.* Biochem Biophys Res Commun, 2006. **351**(4):820-824.